Journal of Materials Chemistry A

Accepted Manuscript

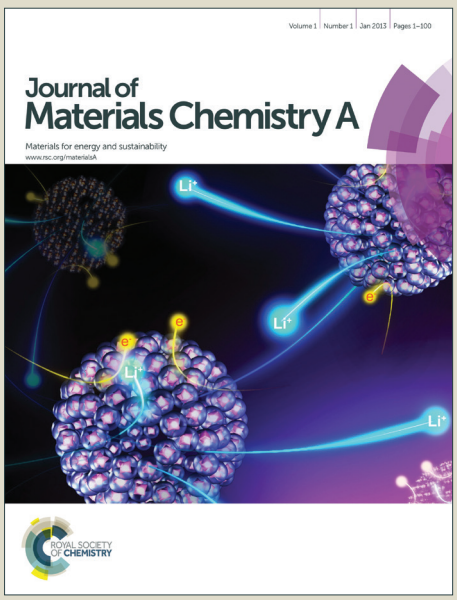

ROYAL SOCIETY OF CHEMISTRY

www.rsc.org/materialsA

Journal of Materials Chemistry A

ARTICLE

Ultra-long Electron Lifetime Induced Efficient Solar Energy Storage by an All-Vanadium Photoelectrochemical Storage Cell Using Methanesulfonic Acid

Received 00th January 20xx,
Accepted 00th January 20xx

DOI: 10.1039/x0xx00000x

www.rsc.org/

Dong Liu, Zi Wei, Syed D Sajjad, Yi Shen and Fuqiang Liu*

The property of supporting electrolyte is critically important to any photo- or electrochemical cells. In this study, we conducted studies and characterization of an all-vanadium photoelectrochemical storage cell (all-V PESC) for highly efficient solar energy storage using methanesulfonic acid (MSA) as a promising supporting electrolyte. Linear sweep voltammetry (LSV) and zero resistance ammetry (ZRA) studies of the all-V PESC show greatly improved photoelectrochemical properties of MSA over conventional H_2SO_4. To elucidate its heightened performance, conductivity and reaction kinetics of the system were investigated by four-probe conductivity measurement and electrochemical impedance spectroscopy (EIS), respectively. EIS results demonstrate vastly reduced charge transfer resistance and interfacial capacitance at the photoelectrode/electrolyte interface via ultra-long photoelectron lifetime; while the conductivity measurement reveals a comparable bulk ionic conductivity to H_2SO_4. Cell efficiency tests indicate a nearly 19-fold enhancement on incident photon-to-electron conversion efficiency (IPCE) and a high Faradaic efficiency (84.8%) in a continuous 60-h operation using MSA as the supporting electrolyte. Besides, multiple cyclic voltammetry (CV) scans on the electrolyte along with XRD and SEM characterization of the photoelectrode both corroborate the exceptional chemical stability of MSA.

Introduction

Solar energy, including radiant light and heat from the sun, has been harnessed by humans since ancient times and the indisputable fact that more energy from sunlight that strikes the earth in one hour than all that consumed by humans in an entire year is the sole driving force for mankind to promote wider and deeper utilization of solar energy.[1] Other than dominant ongoing research and commercialization effort on photovoltaics, and seemingly stagnant progress on photocatalytic/photoelectrochemical fuel generation such as H_2 and methanol, utilizing in-situ characteristics of the photoelectrochemical cell to realize continuous, highly efficient and high output solar energy conversion and storage for large scale applications[2-6] has regained heightened attention in recent years since Licht's success[7] back in 1980s'.

To achieve practically meaningful performance of a photoelectrochemical cell, tremendous attempts have inclined on novel design, surface modification, heterojunction creation, bandgap engineering, nanostructure manipulation, and search of earth-abundant materials for photocatalyst/photoelectrode. However, the state-of-the-art electrode normally requires delicate material synthesis/fabrication and multiple laborious procedures, and is thus time-consuming leave alone less cost-effective. Instead, replacing the supporting electrolyte in a photoelectrochemical cell is a very fast, convenient and inexpensive approach to achieve the goal. Evidently, the ideal supporting electrolyte should possess high ionic conductivity, chemical stability, environmental non-toxicity and low cost compared to existing conventional electrolytes.

Methanesulfonic acid has been widely used as a commercial standard electrolyte in the past three decades to replace the previous industrial standard, fluoroboric acid in many electrochemical processes especially those involving lead and tin.[8] This is due to its excellent physical and chemical properties such as good thermal stability, high water miscibility and metal salts solubility, low relative toxicity, and high conductivity. Furthermore, MSA aqueous solution exposed to open atmospheric conditions could stabilize metal ions in their lower valence states; or, stated differently, MSA solution allows for a unique resistance to the oxidation of metal ions to their higher valence states. In view of these distinguished properties, MSA has been applied to redox flow battery (RFB) research[9-13] lately to improve electrochemical performance. These preliminary studies all reveal its more pronounced thermal stability, metal salt solubility, redox reaction reversibility, improved reaction kinetics and cell efficiencies compared to conventional sulfuric acid. More recently, MSA has been employed as the supporting electrolyte in a photoelectrochemical cell by a group of Polish researchers[14] in combination with WO_3 for photoelectrolysis

Electrochemical Energy Laboratory, Department of Material Science and Engineering, University of Texas at Arlington, Arlington, TX, USA 76019; Email: fuqiang@uta.edu;Tel: +1-817-272-2704; Fax: 814- 272-2538

application. Their results clearly indicate better photoelectrochemical performance achieved by MSA than those by H_2SO_4 or $HClO_4$ on a nanostructured WO_3 photoelectrode.

In this work, MSA was used to replace the commonly employed H_2SO_4 electrolyte in our newly-developed all-vanadium photoelectrochemical storage cell (all-V PESC), and its physical, chemical, electrochemical and photoelectrochemical properties were studied. The results, compared to those achieved under the same conditions using H_2SO_4, show a great potential of MSA as an alternative supporting electrolyte to boost photoelectrochemical performance of the all-V PESC.

Experimental

Electrode Fabrication

TiO_2 photoelectrodes with active area of 1.61 cm^2 were fabricated and used throughout the experiment. To fabricate a TiO_2 electrode, 1.00 g Degussa P25 TiO_2 (Evonik), 2.50 g α-terpineol (Fisher Scientific USA) were mixed under constant stirring at 80°C for 1 h to obtain a uniform TiO_2 slurry. Then the slurry was deposited on a pre-cut square-shaped fluorine doped tin oxide (FTO) (Pilkington USA) using a doctor blade. The FTO substrate was pre-washed with acetone (99.7%, Fisher Scientific USA), methanol (Fisher Scientific USA), and deionized (DI) water several times, before being blow-dried and then further dried in an oven at 120°C for 1 h. The obtained coating was subsequently calcined with air flow at 500°C for 90 min.

Electrolyte Preparation

Six types of electrolytes, including 3 M H_2SO_4 or MSA, 0.01 M vanadium(IV, VO^{2+}) in 3 M H_2SO_4 or MSA, and 0.01 M vanadium(III, V^{3+}) in 3 M H_2SO_4 or MSA, were used in the experiments. The electrolytes were prepared by dissolving specific acids, i.e., H_2SO_4 (J.T. Baker USA) and MSA (Alfa Aesar USA), in DI water with or without vanadium(IV) sulfate oxide hydrate ($VOSO_4 \bullet xH_2O$) (Alfa Aesar USA). The number of water in $VOSO_4 \bullet xH_2O$ was determined by thermogravimetric analysis. The prepared vanadium(IV)-H_2SO_4 and vanadium(IV)-MSA solution both appear light blue. Note that hereafter V-H_2SO_4 and V-MSA refer to vanadium redox in 3 M H_2SO_4 and MSA, respectively. The 0.01 M vanadium(III)-based electrolytes were obtained by electrochemically reducing the prepared vanadium(IV)-based solutions in a three-electrode electrochemical cell at a constant current density of 3 mA/cm^2 using a potentiostat (PARSTAT 2273, Princeton Applied Research) until the potential reached 1.6 V. The electrolyte was protected by N_2 to prevent oxidation of the vanadium(III) species. The obtained vanadium(III)-based electrolytes appear light green.

Material and Cell Characterization

The crystallographic information of the photoelectrode was determined by XRD (Siemens, 810-M340-32-C3000) at a scan rate 0.01°s^{-1} between 20°-80° with a dwell time of 1s. Scanning electron microscopy (Hitachi S-3000N) was used to examine the microstructure of the photoelectrode. The electrochemical and photoelectrochemical properties of the photoelectrode were studied in various electrolytes under dark and/or AM1.5 illumination by linear sweep voltammetry (LSV), cyclic voltammetry (CV), and zero resistance ammetry (ZRA). A two-chamber, three-electrode electrochemical cell was used, where the photoelectrode serves as the working electrode (WE), and a platinum mesh and Ag/AgCl electrode serve as the counter electrode (CE) and reference electrodes (RE), respectively. In a typical experiment, 3 M H_2SO_4/MSA solution with or without 0.01 M V(IV) acid was used as the anolyte, and 3 M H_2SO_4/MSA solution with or without 0.01 M V(III) was used as the catholyte in two chambers of the cell separated by a Nafion 117 membrane. The voltage scan range was from -0.5 to 2.1 V and the scan rate varied from 5 to 20 mVs^{-1}. The overall duration for the ZRA measurement (without any externally applied bias) was 260 s with 20s intervals of alternate dark/illumination. Solar irradiation was created using an ozone-free solar simulator system (Newport USA) coupled with an AM1.5 global filter (Newport USA) and calibrated using a standard photodiode (Newport USA).

The electrochemical impedance spectroscopy (EIS) was used to probe bulk electrolyte conductivity at room temperature (25 °C) and photoelectrochemical reaction kinetics of the cell. All data were recorded at open-circuit voltage (OCV) over a frequency range from 1 mHz to 2 MHz with an amplitude of 10 mV. Nyquist plots using various electrolytes were also used to determine ohmic resistance of the cell and the ionic conductivity of bulk electrolyte was calculated according to the following equation[15]:

$$\boldsymbol{\sigma} = \frac{\boldsymbol{L}}{\boldsymbol{Z_{re} \cdot A}} \quad (1)$$

where σ is the ionic conductivity of bulk electrolyte, L is the overall length of four sensing probes (1.33 cm), Z_{re} is ohmic resistance of the cell and A is the electrode area (1.72 cmx0.12 cm) available for ionic conduction. Note that such ohmic resistance obtained from the Nyquist plot only contains the contribution of the electrolyte and sensing electrodes. As the contribution of the latter can be considered insignificant, the resistance of the cell is therefore approximated as the resistance of the electrolyte.

Nyquist plot and Bode plot of EIS were both employed to reveal electron lifetime of the photoelectrode during the reaction. By using the following semi-empirical equation,[16-18] the numerical value of photoelectron lifetime in various electrolytes can be calculated.

$$\boldsymbol{\tau_e} = \frac{\boldsymbol{1}}{\boldsymbol{2\pi f_{max}}} \quad (2)$$

where τ_e is the lifetime of photogenerated electrons and f_{max} is the maximum frequency of the peak in the low frequency region.

To measure incident photon-to-current conversion efficiency (IPCE) of the cell, the wavelength of the incident

light was controlled by a monochromator (Edmund Optometrics) from 200 to 600 nm in combination with the following equation[19]:

$$IPCE = \frac{1240 \cdot I_{ph}}{\lambda \cdot J_{light}} \quad (3)$$

where I_{ph} is the measured photocurrent density at a specific wavelength, λ is the wavelength of incident light, and J_{light} is the light irradiance determined by a photodetector (Newport, USA).

Faradaic efficiency (η_F) is calculated by the following equation

$$\eta_F = \frac{F \cdot \Delta n}{\Delta Q} \quad (4)$$

where Δn is the amount of reacted vanadium redox species during the cell operation, F is the Faraday's constant as 96485 C/mol, and ΔQ is the charge transferred during the cell operation.

The concentration of vanadium redox species was determined by assaying a small amount (~10 ml) of the electrolyte using a quartz cuvette with a fixed path length (1 cm) in a UV–vis spectrophotometer (PerkinElmer Lambda 35). According to Beer-Lambert law shown below, a linear relationship can be assumed between the absorbance at the characteristic peak of vanadium redox and its concentration.

$$A = \varepsilon l c \quad (5)$$

where ε is molar absorptivity of the sample measured, l is the path length of the cuvette in which the sample is contained, and c is the concentration of the vanadium redox species.

Results and Discussion

Photoelectrochemical Study

Fig. 1 presents the photoelectrochemical performance of the cell studied by LSV and ZRA using a TiO_2 photoelectrode in various electrolytes under dark and AM1.5 illumination. It is shown in Fig. 1a that MSA leads to a four-fold improvement in photocurrent in comparison to H_2SO_4. Considering the fact that the concentration of MSA used in our experiments is very high, corresponding to a negative pH value of the electrolyte, the above preliminary results render MSA a very promising electrolyte for photoelectrochemical solar energy conversion and storage. Also note that the oxidation peak near -0.1 V at the beginning of the scan is associated with the so-called *Brutto* reaction, i.e., a charge compensating reaction of TiO_2 in acidic aqueous electrolyte. Study of this reaction will be detailed in later section of this work.

In order to further investigate photoelectrochemical performance of MSA, the cell was studied using ZRA method (no external bias applied) in contrast to LSV and the results are shown in Fig. 1b. As seen in the figure, pure MSA is chemically stable upon illumination and it shows significantly enhanced photocurrent (5 times higher) than that in pure H_2SO_4 within the entire test window under AM1.5 illumination. Albeit

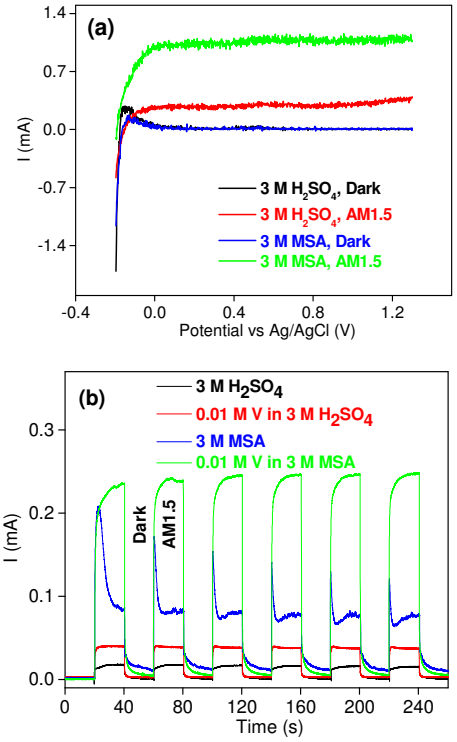

Fig.1. Photoelectrochemical behaviour of the photoelectrochemical cells studied by (a) linear sweep voltammetry at 5 mV/s and (b) zero-resistance ammetry using TiO_2 photoelectrode in various electrolytes under dark and AM1.5 illumination. Only pure acid was used in Fig. 1a, whereas vanadium redox species were involved in Fig. 1b where vanadium(IV, VO^{2+}) and vanadium(III, V^{3+}) serve as the anolyte and catholyte, respectively. Electrode reactions at the photoanode and Pt cathode follow: $VO^{2+} + H_2O \rightarrow VO_2^+ + e^- + 2H^+$ and $V^{3+} + e^- \rightarrow V^{2+}$, respectively.

current spikes, attributed to surface trap states of TiO_2, were observed at the beginning upon illumination, the photocurrent reaches equilibration eventually after a short period of time.

This result is in alignment with the above LSV findings and it further justifies MSA as a promising electrolyte for photoelectrochemical solar energy conversion and storage. What's worth mentioning in Fig. 1b is that MSA gives even higher photocurrent than the V-H_2SO_4 electrolyte on a TiO_2 photoelectrode, which may indicate its greater ability of MSA to enhance photoelectrochemical reaction and prevent charge recombination. Consequently, it is suspected and confirmed in Fig. 1b that V-MSA would show even more improved photoelectrochemical performance. When vanadium redox species are present in the electrolyte, an all-V PESC is formed. Upon illumination, photogenerated holes and electrons from TiO_2 tend to react with VO^{2+} in the anolyte chamber and V^{3+} in the catholyte chamber respectively, providing the photocurrent while converting solar energy to chemical energy simultaneously. The stored chemical energy can be released by reversing the reactions upon demand. It is seen in Fig. 1b that the photocurrent of TiO_2 is boosted almost 7 times than that in

V-H_2SO_4 electrolyte under the same concentrations of vanadium redox species. We ascribe the photocurrent enhancement to the synergistic effect of MSA and fast reaction kinetics of vanadium redox species. Note that two different ZRA profiles emerged depending on the electrolyte used. The ZRA profiles using H_2SO_4, V-H_2SO_4 and V-MSA resemble each other, showing gradually increased photocurrent while the one using MSA shows gradually declined photocurrent till equilibration. Actually, other than the initial photocurrent spikes upon illumination, the ZRA profile using pure MSA as the electrolyte (blue line) also shows a gradually increased photocurrent after ca. 1/6 of the illumination period till equilibration. Thus it is more scientifically sound to use ZRA profile after the photocurrent reaches equilibration. In addition, noticeable residual dark current was observed on MSA-based electrolytes but not on H_2SO_4-based electrolytes in Fig. 1b and this interesting phenomenon in connection with other results will be elaborated in later section of this study.

Bulk Ionic Conductivity Study

As demonstrated by both LSV and ZRA results, MSA exhibits much more superior photoelectrochemical performance compared to conventional H_2SO_4. To unfold the root cause of its better performance, a more detailed study with respect to its physical property and reaction kinetics was implemented.

We started first by studying the ionic conductivity of bulk electrolyte using EIS and four-probe electrical conductivity measurement. It is already reported[8] that conductivity of 1.0 $molL^{-1}$ MSA aqueous solution (0.30 Scm^{-1}), is comparable to those of hydrochloric acid (0.35 Scm^{-1}) and sulfuric acid (0.44 Scm^{-1}), yet posing a lower risk of corrosion compared with other mineral acids. We speculate even greater conductivity of MSA-based electrolytes especially under much higher concentration.

Table 1 depicts calculated ionic conductivity of various electrolytes based upon corresponding ohmic resistance of the cell obtained by EIS. As seen in the table, all electrolytes show very similar ionic conductivity values. In contrast to pure H_2SO_4, pure MSA has slightly smaller bulk ionic conductivity but within the same order of magnitude. This result is consistent with the discovery reported in the literature.[8, 14] Ionic conductivity in electrolytes depends on two main factors: (i) the concentration of ions and (ii) the mobility of ions under an electric field. Since both MSA and H_2SO_4 are strong acids with similar pK_a values (-1.92 and -3 for the former and latter, respectively), the observed slightly lower conductivity of MSA may be solely attributed to its lower mobility (bulkier) of MSA anions. Meanwhile, the ionic conductivity of both electrolytes increases after vanadium ions are involved in the solution and this is ascribed to the additional contribution from vanadium cations according to classic Kohlrausch's law[20] which states that conductivity of a strong electrolyte solution is equal to the sum of conductivity contributions from the cation and anion.

Table 1.Calculated ionic conductivity of various electrolytes.

Electrolytes	Ohmic Resistance (Ω)	Conductivity(S/cm)
3 M H_2SO_4	0.9487	5.8972
0.01 M V-H_2SO_4	0.8149	6.8655
3 M MSA	1.1158	5.0141
0.01 M V-MSA	0.9621	5.8151

Electrochemical Impedance Spectroscopy Study

EIS was also employed to investigate reaction kinetics of the cell using MSA-based electrolytes given our previous success.[21] Fig.2 represents (a) Nyquist plots and (b) Bode plots of a TiO_2 photoelectrode in various electrolytes under AM1.5 illumination. As seen in Fig. 2a, one semi-circle at high frequency and one arc/partial arc at mid frequency were observed in all tested electrolytes. The semi-circle at high frequency corresponds to electron transport resistance and interfacial capacitance at the Pt/electrolyte interface while the arc/partial arc at mid frequency represents charge transfer resistance and interfacial capacitance at the TiO_2/vanadium(IV) redox interface. It is clear that all electrolytes have little influence on electron transport resistance and interfacial capacitance at Pt/electrolyte interface as they all show very similar value ~50 Ω (inset of Fig. 2a).

However, great difference is seen at the TiO_2/electrolyte interface, depending on the selection of electrolyte. The cell using 3 M H_2SO_4 electrolyte shows the mid frequency arc with the biggest diameter compared to others and this is indicative

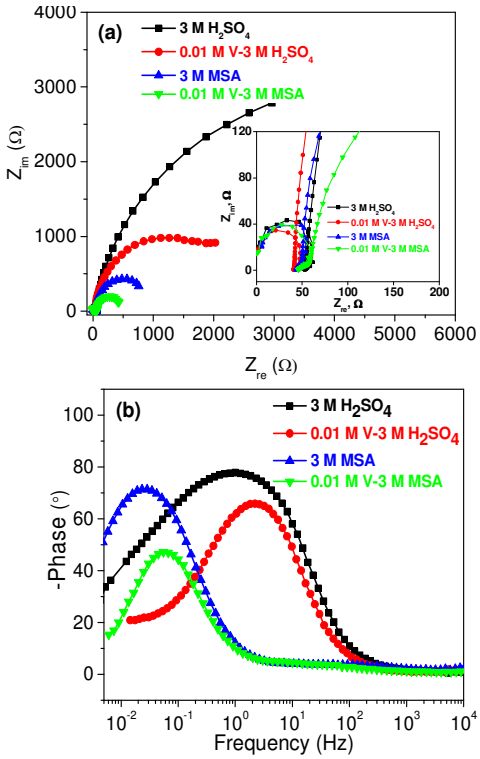

Fig. 2. (a) EIS Nyquist plots and (b) Bode plots of the cells using TiO_2 as the photoelectrode in various electrolytes under AM1.5 illumination.

of slow kinetics of water splitting reactions. When vanadium redox is involved in the electrolyte, charge transfer resistance and interfacial capacitance at the TiO_2/electrolyte interface are reduced greatly due to fast reaction kinetics of vanadium redox, in good agreement with what was already revealed in our previous work.[21-23] The same argument can be applied to MSA electrolyte as well. Other than that, MSA-based electrolytes exhibit much smaller charge transfer resistance and interfacial capacitance than H_2SO_4-based electrolytes regardless of vanadium redox participation at the TiO_2/electrolyte interface. Especially, the 0.01 M V-MSA electrolyte displays approximately 5 times smaller resistance compared to the 0.01 M V-H_2SO_4. These results are in great agreement with the LSV and ZRA results, further proving that MSA holds a great potential as an encouraging electrolyte in photoelectrochemical solar energy conversion and storage.

Bode plots in Fig. 2b were further utilized to shed light on the lifetime of photogenerated electrons in the reaction. Clear difference from all electrolytes is seen in Fig.2b. Peaks given by the two MSA-based electrolytes despite of vanadium redox, both shift to lower frequency region by two orders of magnitude compared to their counterparts in H_2SO_4 electrolyte. This graphically indicates that the photoelectron lifetime in MSA-based electrolyte is significantly prolonged compared to it in H_2SO_4-based electrolytes. Table 2 lists calculated electron lifetime of a TiO_2 photoelectrode in various electrolytes under AM1.5 illumination based upon the measured maximum frequency from EIS. It is seen that the MSA-based electrolytes on one hand, display astonishingly longer electron lifetime compared to the H_2SO_4-based electrolytes. Specifically, pure MSA and V-MSA electrolytes are capable of prolonging electron lifetime by a factor of 43 and 40 compared to their H_2SO_4 counterparts, respectively. Geraldine et al[24] discovered that MSA has a preference to adsorb at the surface of aqueous solutions so that a tight electrostatic double layer structure tends to form between MSA and water molecules, as a result of ionic interactions between surface methanesulfonicate anions and H_3O^+ or $H_5O_2^+$ cations. Thus it is highly plausible that the tremendously long electron lifetime arises from the strong charge extraction of such tight electrostatic double layer between MSA and water molecules.

One the other hand, vanadium redox seems to play an important role by reducing electron lifetime on TiO_2 photoelectrodes and this is true for both H_2SO_4 and MSA. We ascribe this to quick charge scavenging ability of vanadium redox due to its fast reaction kinetics. These significantly scavenged charge carriers contribute greatly to the high photocurrent. As a result, although electron lifetime of the TiO_2 electrode is shortened vastly in vanadium-based electrolytes compare to that in pure acid electrolytes, fast reaction kinetics of vanadium species still surpasses this effect to produce higher photocurrents, as indicated in all our previous studies[6, 21-23] and in Fig. 1b. As a comparison, the ratio of electron lifetime in vanadium-based electrolytes to that in pure acid electrolytes for both H_2SO_4 and MSA were calculated. The values of 0.45 and 0.43, respectively, are very close to each other, implying the same electrochemical and/or photoelectrochemical behaviour of vanadium redox in two different acids. These result and analysis are in good agreement with the previous LSV and ZRA results, indicating a greatly diminished charge carrier recombination and better photocatalytic property of MSA electrolyte, especially in the presence of vanadium redox species. The origin of the observed enhancement may root from possible interaction between MSA and charge carriers or/and vanadium ions. The interaction between MSA and actinide ions, particularly oxygenated cations, has already been reported.[25] The interaction could arise from electron donating nature of the methyl group in MSA, which helps stabilize possible reaction intermediates in the photoelectrochemical process and thus improve the photocurrent.

Furthermore, the significantly prolonged electron lifetime by MSA may also explain the noticeable dark currents for the MSA-based electrolytes in Fig. 1b, while H_2SO_4 reveals no sign of charge carrier adsorption by flattening out the dark current. It is suspected that such dark current of MSA is due to large amount of uncompensated charge carrier adsorption at the semiconductor/liquid interface immediately after light off. These uncompensated charge carriers, however, can be eliminated by discharging the cell under dark for extended period of time according to our preliminary experiments. This is also in good agreement with the above-mentioned discussion regarding the role of vanadium species, which is illustrated in Fig. 1b by the reduced dark current as the vanadium redox helps reduce electron lifetime considerably through scavenging uncompensated charge carriers at the TiO_2/electrolyte interface.

Table 2. The maximum frequency of the peak and calculated electron lifetime of a TiO_2 photoelectrode in various electrolytes under AM1.5 illumination.

Electrolytes	f_{max} (Hz)	τ_e (ms)
3 M H_2SO_4	1	159.2
0.01 M V-H_2SO_4	2.205	72.2
3 M MSA	0.0235	6775.9
0.01 M V-MSA	0.055	2895.2

Efficiency Study

The cell efficiencies of an all-V PESC such as IPCE and Faradaic efficiency by using MSA-based electrolytes were investigated to quantitatively reveal its photoelectrochemical performance. The IPCE of the storage cell using various electrolytes is shown in Fig. 3. All curves show a maximum efficiency at 350 nm regardless of the electrolyte, which is attributed to the large bandgap of TiO_2 that absorbs only UV light. Pure H_2SO_4 electrolyte, as demonstrated in our previous study[6], only gives a low IPCE value of 2.45% due to slow reaction kinetics of water splitting reaction, whereas pure MSA electrolyte improves cell IPCE more than 7 times. On the other hand, vanadium redox, as expected, plays a significant role by boosting IPCE of the cell, especially in the MSA electrolyte.

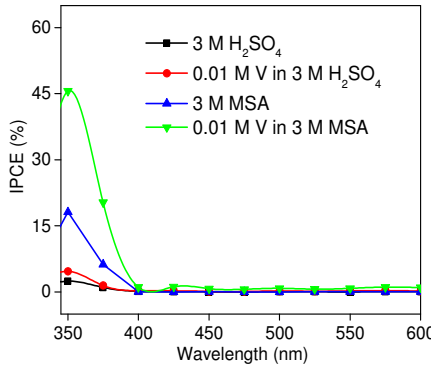

Fig.3. IPCE of the cells using a TiO_2 photoelectrode in various electrolytes.

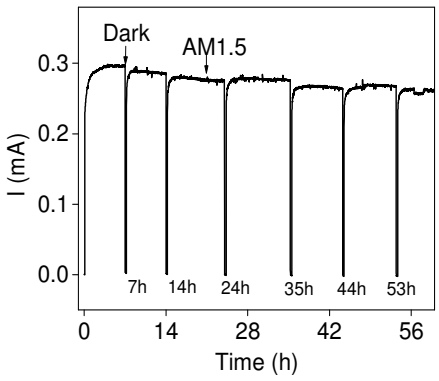

Fig. 4. The 60-h photocurrent profile of an all-V PESC using TiO_2 photoelectrode and 0.01 M V- MSA electrolytes under AM1.5 illumination. A ZRA test protocol was used through the test.

With vanadium redox in the electrolyte, IPCE of the cell is doubled for the H_2SO_4-based electrolyte. When H_2SO_4 is replaced with MSA as the supporting electrolyte, the highest value (45.6%) is achieved with the assistance of vanadium redox, improving IPCE of the cell by a factor of 18.6, 9.7, and 2.5 compared to pure H_2SO_4 acid, 0.01 M V-H_2SO_4, and pure MSA electrolyte, respectively. Such remarkable IPCE enhancement of the cell is believed to result from a strong synergy between fast vanadium redox kinetics and prolonged electron life time induced by MSA. These results are in agreement with the previous LSV, ZRA and EIS results.

To calculate Faradaic efficiency, the cell must be operated under a prolonged period of time, which not only renders as an indicator of chemical stability of the cell, but also induces observable concentration change of vanadium redox as a result of solar energy conversion and storage. Fig. 4 illustrates a 60-h photocurrent profile of an all-V PESC using a TiO_2 photoelectrode in 0.01 M V-MSA electrolyte under AM1.5 illumination. The cell displays very stable photocurrent throughout the whole test window, although slight fluctuation caused by intentional interruption of the light at different period of time is observed. After 60-h cell operation, the photocurrent retention still remains 89.5%, which indicates a great chemical stability of the cell with high photoelectrochemical performance.

The slight photocurrent loss may be due to: (i) concentration polarization loss of vanadium redox species in the electrolyte during the long-term test; (ii) trivial physical destruction of photoelectrode confirmed by observed slight delamination of TiO_2 from the surface of FTO substrate after the test. For only the demonstration purpose, our photoelectrode was fabricated more like a coating rather than a thin film. When the photoelectrode is immersed in the liquid for as long as 60 h, slight delamination occurs naturally as the liquid electrolyte tends to swell the solid from FTO substrate. This mild electrode physical destruction can be greatly and easily improved to mitigate photocurrent loss by advanced thin film fabrication techniques, such as electrochemical deposition, chemical vapor deposition (CVD), pulsed laser deposition (PLD) or physical vapor deposition (PVD) etc.

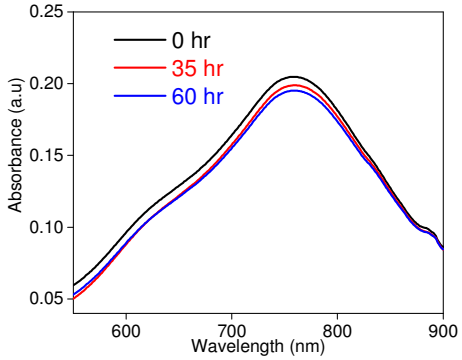

Fig.5. UV-vis absorbance spectra of the electrolyte in the anolyte chamber at different periods of time during a 60-h continuous cell operation.

Recently, UV-vis spectroscopy has been successfully developed[26-29] to monitor state of charge (SOC) of redox flow batteries; such method was also utilized in our study to monitor the electrolyte concentration change before and after the cell operation. Fig. 5 shows the absorbance change of vanadium(IV) ions (VO^{2+}) in the beginning, the middle, and the end of the 60-h cell operation as demonstrated in Fig. 4. With increasing time, the vanadium(IV) ion concentration starts to decrease, indicating more and more VO^{2+} ions are converting to VO_2^+ ions by photogenerated charge carriers, i.e., holes, in the anolyte chamber. Assuming a linear relationship between the absorbance at the characteristic peak (765 nm) of VO^{2+} and concentration, i.e., the Beer's Law, Faradaic efficiency is then calculated to be 84.8% according to Eq. 4. It is suspected that possible side reactions, such as hydrogen evolution reaction (HER) and oxygen evolution reaction (OER), are likely to occur. This is because the electrochemical potential of H_2/H_2O is more positive than TiO_2 conduction band position while that of O_2/H_2O is more negative than TiO_2 valence band position, which serves as the driving force to split water photoelectrochemically. However, the fast reaction kinetics of vanadium redox ($\sim 10^6$ times higher exchange current density

than those of oxygen reduction/evolution reactions according to our preliminary calculation) would be expected to mitigate these side reactions appreciably, thus contributing little to Faradaic efficiency loss.

Stability Study

Finally, the chemical stability of the system, especially with respect to both photoelectrode and electrolyte, was studied. CV was employed to investigate the chemical stability of MSA while the all-V PESC was in operation. Fig. 6 shows the cyclic voltammograms of the cell using pure MSA as the electrolyte in conjunction with a TiO_2 photoelectrode under a large scan range of voltage.

Fifty scans were conducted on the cell under alternate dark and AM1.5 illumination conditions. As shown in the graph, TiO_2 shows a typical n-type semiconductor photoelectrochemical behaviour in the MSA electrolyte. Within the scan range, no other oxidation/reduction peak other than the one near -0.11V is observed on anodic scans. This peak is ascribed to the charge that compensates proton adsorption or intercalation reaction in TiO_2 in acidic aqueous electrolyte[30-32] and is described by the following *Brutto* reaction:

$$Ti^{IV}O_2 + e^- + H^+ \leftrightarrow Ti^{III}OOH$$

In addition, above 2.0V, the current starts to increase rapidly due to sufficient overpotential being provided to split water with fast reaction rate, either electrolytically (under dark) or photoelectrolytically (under illumination). The results shown in Fig. 6 confirm that MSA is a chemically stable supporting electrolyte to participate in electrochemical and photoelectrochemical reactions, as corroborated by Fig. 4.

XRD and SEM were also performed on the TiO_2 photoelectrode after the 60-h cell operation demonstrated in Fig. 4 to examine crystal structure/phase change and morphology change associated with the cell operation. The XRD result shown in Fig. 7a clearly indicates that the crystal

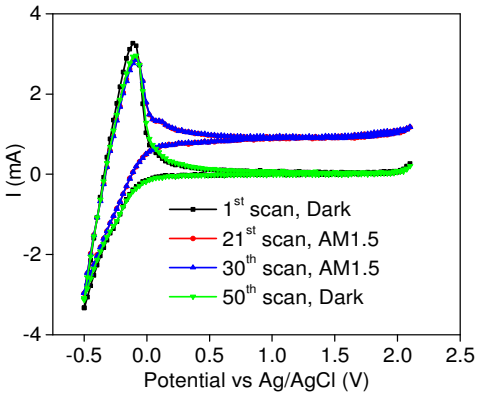

Fig. 6. Cyclic voltammogramsof the cell using pure MSA as the electrolyte and TiO_2 as the photoelectrode with a scan range from -0.5 to 2.1V under dark and AM1.5 illumination. The scan rate is 20 mV/s.

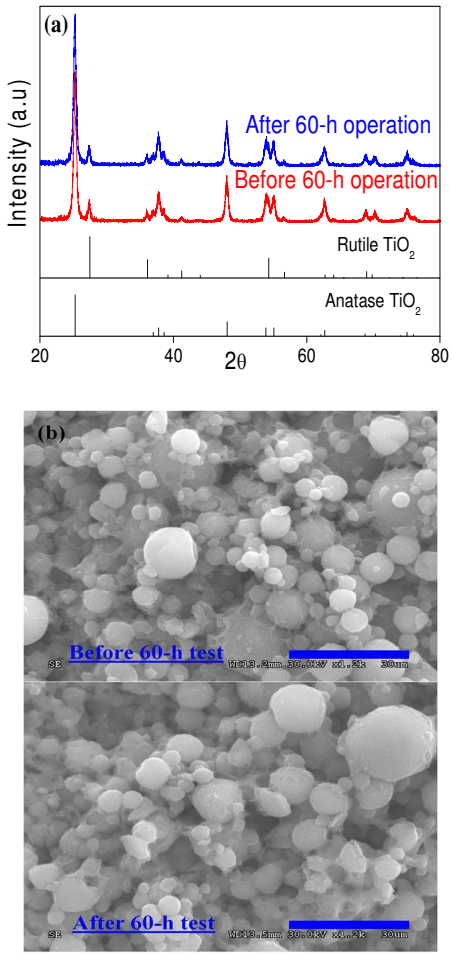

Fig.7. XRD (a) and SEM (b) characterization of TiO_2 photoelectrode used in Fig. 4 before and after the 60-h photoelectrochemical test. The scale bar is 30 um in the SEM images.

structure of TiO_2 remains unchanged when in contact with MSA during the 60-h test. Only anatase and rutile phases of TiO_2 are observed, and no impurity is detectable after the long-term test. SEM images of TiO_2 photoelectrode revealed in Fig. 7b further corroborate with XRD findings. After 60-h cell operation, negligible difference was observed on the morphology of TiO_2 particle. Note that the rough surface and minor craters/irregularities of TiO_2 were caused by heat treatment, which is in line with our previous findings.[23] Herein, we have concluded that the system, particularly the photoelectrode and MSA-based electrolyte, is chemically and photoelectrochemically stable with the promise of offering high solar energy storage efficiency and capacity.

Conclusions

The electrochemical and photoelectrochemical properties of MSA were investigated in an all-V PESC by conductivity measurements, LSV, CV, ZRA, and EIS. LSV studies reveal 4 times higher photocurrent using pure MSA than H_2SO_4; while

studies using ZRA, in alignment with those of LSV, demonstrate that MSA is capable of boosting the photocurrent approximately by a factor of 7 when vanadium redox species are involved. Although the bulk ionic conductivity of MSA-based electrolytes is found to be closely comparable to that of H_2SO_4-based electrolytes, EIS Nyquist plots, however, reveal that MSA greatly diminishes charge transfer resistance and interfacial capacitance at the photoelectrode/electrolyte interface under illumination, especially when vanadium redox species participates in the reactions. Besides, EIS Bode plots manifest that remarkably longer electron lifetime is realized in photoelectrochemical reactions using MSA-based electrolytes compared to H_2SO_4-based ones though vanadium redox species shorten electron lifetime in both acids due to its quick charge-scavenging ability. The peak IPCE achieved on V-MSA electrolyte (at 45.6%), which is 18.9, 9.7 and 2.5 times higher than those achieved using pure H_2SO_4, V-H_2SO_4, and pure MSA electrolytes respectively, is attributed to the synergistic effect of fast reaction kinetics of vanadium redox and prolonged electron life time of MSA. After a 60-h cell operation, Faradaic efficiency of the all-V PESC was calculated to 84.8%. Furthermore, multiple CV scans show that MSA is chemically and electrochemically stable in a large potential window under both dark and illumination conditions, and XRD and SEM characterization show no crystal structure and morphology change of the TiO_2 photoelectrode even after a 60-h cell operation.

Acknowledgements

All authors are grateful for the financial support from National Science Foundation Career Award under Grant Number ECCS-1254915.

Notes and references

1 N. S. Lewis, *Science*, 2007, **315**, 798-801.
2 P. Liu, Y.-l. Cao, G.-R. Li, X.-P. Gao, X.-P. Ai and H.-X. Yang, *ChemSusChem*, 2013, **6**, 802-806.
3 N. F. Yan, G. R. Li and X. P. Gao, *J.Electrochem. Soc.*, 2014, **161**, A736-A741.
4 M. Yu, X. Ren, L. Ma and Y. Wu, *Nat. Commun.*, 2014, **5**.
5 N. F. Yan, G. R. Li and X. P. Gao, *Journal of Materials Chemistry A*, 2013, **1**, 7012-7015.
6 Z. Wei, D. Liu, C. Hsu and F. Liu, *Electrochem.Commun.*, 2014, **45**, 79-82.
7 S. Licht, G. Hodes, R. Tenne and J. Manassen, *Nature*, 1987, **326**, 863-864.
8 M. D. Gernon, M. Wu, T. Buszta and P. Janney, *Green Chem.*, 1999, **1**, 127-140.
9 C. Tang and D. Zhou, *Electrochim. Acta*, 2012, **65**, 179-184.
10 P. K. Leung, M. R. Mohamed, A. A. Shah, Q. Xu and M. B. Conde-Duran, *J. Power Sources*, 2015, **274**, 651-658.
11 S. Peng, N-F. Wang, X-J Wu, S-Q. Liu, D. Fang, Y-N. Liu, K-L. Huang, *Int. J.Electrochem. Sc.*, 2012, **7**, 643-649.
12 Z. He, Z. Li, Z. Zhou, F. Tu, Y. Jiang, C. Pan and S. Liu, *IRESR*, 2013, **5**, 023130.
13 G. Wang, J. Chen, X. Wang, J. Tian, H. Kang, X. Zhu, Y. Zhang, X. Liu and R. Wang, *J. Energy Chem.*, 2014, **23**, 73-81.
14 R. Solarska, R. Jurczakowski and J. Augustynski, *Nanoscale*, 2012, **4**, 1553-1556.
15 J. A. Bard, Faulkner, R. L., *Electrochemical Methods: Fundamentals and Applications*, Wiley, 2000.
16 D. Kuang, P. Wang, S. Ito, S. M. Zakeeruddin and M. Grätzel, *J. Am. Chem. Soc.*, 2006, **128**, 7732-7733.
17 C. Cheng, W. Ren and H. Zhang, *Nano Energy*, 2014, **5**, 132-138.
18 Q. Wang, J.-E. Moser and M. Grätzel, *J. Phys. Chem. B*, 2005, **109**, 14945-14953.
19 A. B. Murphy, P. R. F. Barnes, L. K. Randeniya, I. C. Plumb, I. E. Grey, M. D. Horne and J. A. Glasscock, *Int. J. Hydrogen Energy*, 2006, **31**, 1999-2017.
20 G. Clinton, *Further Light on the Theory of the Conductivity of Solutions*, The Chemical Publishing Co., Easton, PA, 1921.
21 D. Liu, W. Zi, S. D. Sajjad, C. Hsu, Y. Shen, M. Wei and F. Liu, *ACS Catal.*, 2015, **5**, 2632-2639.
22 D. Liu, F. Liu and J. Liu, *J. Power Sources*, 2012, **213**, 78-82.
23 D. Liu, Z. Wei, C.-j. Hsu, Y. Shen and F. Liu, *Electrochim. Acta*, 2014, **136**, 435-441.
24 H. C. Allen, E. A. Raymond and G. L. Richmond, *J. Phys. Chem. A*, 2001, **105**, 1649-1655.
25 G. B. Andreev, N. A. Budantseva, I. G. Tananaev and B. F. Myasoedov, *Radiochemistry+*, 2009, **51**, 225-230.
26 Z. Tang, D. S. Aaron, A. B. Papandrew and T. A. Zawodzinski, *ECS Trans.*, 2012, **41**, 1-9.
27 X. Gao, R. P. Lynch, M. J. Leahy and D. N. Buckley, *ECS Trans.*, 2013, **45**, 25-36.
28 R. P. Brooker, C. J. Bell, L. J. Bonville, H. R. Kunz and J. M. Fenton, *J. Electrochem. Soc.*, 2015, **162**, A608-A613.
29 M. Skyllas-Kazacos and M. Kazacos, *J. Power Sources*, 2011, **196**, 8822-8827.
30 M. Zukalova, M. Bousa, Z. Bastl, I. Jirka and L. Kavan, *J. Phys. Chem. C*, 2014, **118**, 25970-25977.
31 T. Berger, T. Lana-Villarreal, D. Monllor-Satoca and R. Gómez, *Electrochem.Commun.*, 2006, **8**, 1713-1718.
32 H. Pelouchova, P. Janda, J. Weber and L. Kavan, *J. Electroanal. Chem.*, 2004, **566**, 73-83

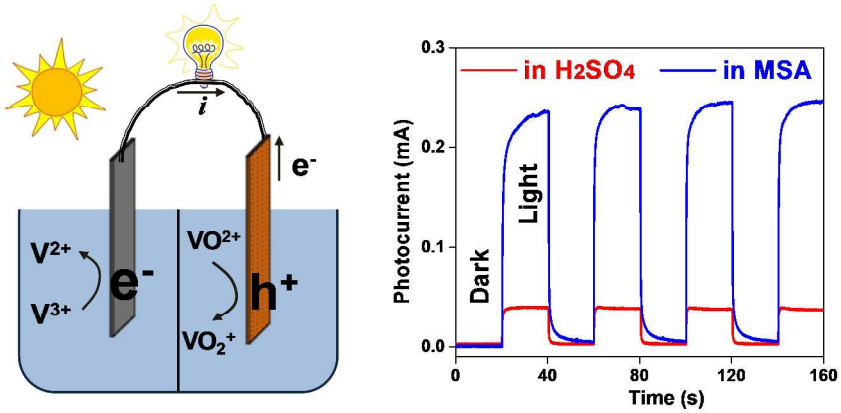

An all-vanadium photoelectrochemical storage cell (PESC) using methanesulfonic acid (MSA) shows superior photoelectrochemical performance in solar energy storage.